Applied Energy 372 (2024) 123834

Contents lists available at ScienceDirect

Applied Energy

journal homepage: www.elsevier.com/locate/apenergy

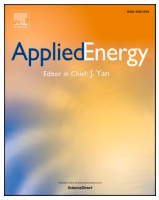

# Indicators for suitability and feasibility assessment of flexible energy resources

Pablo Calvo-Bascones [a,b,*], Francisco Martín-Martínez [b]

[a] Faculty of Economics and Business Administration (ICADE), Universidad Pontificia Comillas, Madrid, Spain
[b] Institute for Research in Technology, Universidad Pontificia Comillas, Madrid, Spain

## HIGHLIGHTS

- Determine flexible end-users based on energy level, consistency and variability.
- Rank the topology based on high resolution 3D models to assess radiation levels based on angle, orientation and structural singularities.
- Combination of both indicators through and hybrid approach
- Assessment of suitability and feasibility of potential end-users with PV energy sources.

## ARTICLE INFO

*Keywords:*
Indicators
Demand side management
Solar energy
Decision support systems
Building topology

## ABSTRACT

Recommender systems play a critical role in optimizing building energy consumption by providing personalized advice based on data analytics and user preferences. However, the literature highlights the need for systems that can justify their recommendations, as many of these systems use non-transparent machine-learning techniques. This research introduces two distinct types of indicators with three main goals: to identify patterns of flexible consumption behavior using transparent and straightforward methods suitable for remote decision support systems, thereby eliminating the need for extensive databases; to evaluate the feasibility of installing solar panels on building facades, rooftops, and structures using high-resolution 3D models; and to enhance understanding through a quantitative assessment of the feasibility and suitability of integrating renewable energy sources, particularly photovoltaic systems. Flexible prosumers are scored by assessing their energy consumption level, consistency, and variability through the Flexible Consumption Indicators. Topology Indicators perform a quantitative assessment of the feasibility of support surfaces for installing photovoltaic panels, taking into account rooftop pitch angles, orientations, and surrounding and internal structures, identifying those areas exposed to sufficient levels of irradiation. This study, which uses actual consumption profiles and similar households' buildings 3D models, demonstrates how the proposed indicators can aid identifying users with flexible consumption profiles that reside in buildings compatible with renewable energy sources, aiding in decision-making process within the energy transition.

## 1. Introduction

Energy consumption in buildings plays a critical role in the overall energy landscape and the transition to a sustainable future. Buildings account for 40% of global energy consumption [1]. As the world faces the challenges of climate change and the need to reduce carbon emissions, optimizing energy consumption through Demand Response (DR) actions and efficiency in buildings becomes critical, as seen in policies such as the European Green Deal [2]. The widespread adoption of solar production in buildings [3,4] can substantially decrease CO2 emissions associated with electricity generation, contributing to Europe's commitment to reducing carbon footprints. As highlighted by [5], people willing to change their appliances (energy efficiency) or install new devices (automatic DR or photovoltaic (PV) adopters) are also ready to change their energy behavior (manual DR). Thus, PV adopters and flexible users are interdependent.

The year 2022 witnessed a remarkable surge in PV energy generation, with a historic increase of 270 TWh (up 26%), culminating in nearly 1300 TWh. This notable achievement not only marked the most

* Corresponding author at: Faculty of Economics and Business Administration (ICADE), Universidad Pontificia Comillas, Madrid, Spain
*E-mail addresses:* pcalvo@comillas.edu (P. Calvo-Bascones), francisco.martin@iit.comillas.edu (F. Martín-Martínez).

https://doi.org/10.1016/j.apenergy.2024.123834
Received 8 May 2024; Received in revised form 14 June 2024; Accepted 30 June 2024
Available online 8 July 2024
0306-2619/© 2024 The Authors. Published by Elsevier Ltd. This is an open access article under the CC BY-NC-ND license (http://creativecommons.org/licenses/by-nc-nd/4.0/).

**Nomenclature**

*Abbreviations*

| | |
|---|---|
| 2D/3D | Two/Three dimensional |
| ALI | Amplitude Level Indicator |
| DL | Deep Learning |
| DR | Demand Response |
| DSO | Distribution System Operator |
| ECI | Energy Consistency Indicator |
| ELI | Energy Level Indicator |
| EVI | Energy Variation Indicator |
| FEI | Feasible Exposure Indicator |
| $I_1$ | Flexible Consumption Indicator, a total indicator that aggregates the five consumption indicators. |
| $I_2$ | Topology Indicator, a total indicator that aggregates the three topology indicators. |
| $I_{TOT}$ | The final indicator is an aggregation of $I_1$ and $I_2$, which can be calculated using a geometric, an arithmetic, or a hybrid (mixed) approach combining both methods. |
| ML | Machine Learning |
| NILM | Non-intrusive load monitoring |
| OI | Orientation Indicator |
| PV | Photovoltaic |
| RPI | Roof Pitch Indicator |
| SDI | Standard Deviation Indicator |

*Parameters and Variables used in algorithms*[11]

| | |
|---|---|
| C | Time series containing power consumption (kW) D days and T values |
| d, D | d is an auxiliary variable that indicates the day of set D. |
| t, T | t is an auxiliary variable that indicates the time of the set T. |
| Y[1:D] [1:T] | Matrix of power consumption (kW) per day and time value |
| E[1:D] | Vector of energy (kWh) per day |
| z | Auxiliary variable used to build indicators |
| L, H | Parameters used to establish levels in the grading of the different algorithms. |
| M[1:T] | Vector of Mean power consumption (kW) per period T |
| S[1:T] | Vector of Standard deviation of the power consumption (kW) per period T |
| M | Mean of the daily energy (kWh) |
| S | Standard deviation of the daily energy (kWh) |
| Qx[1:T] | Vector of the quartile x of the power consumption (kW) per period T |
| R[1:T] | Vector of interquartile ranges of the power consumption (kW) per period T |

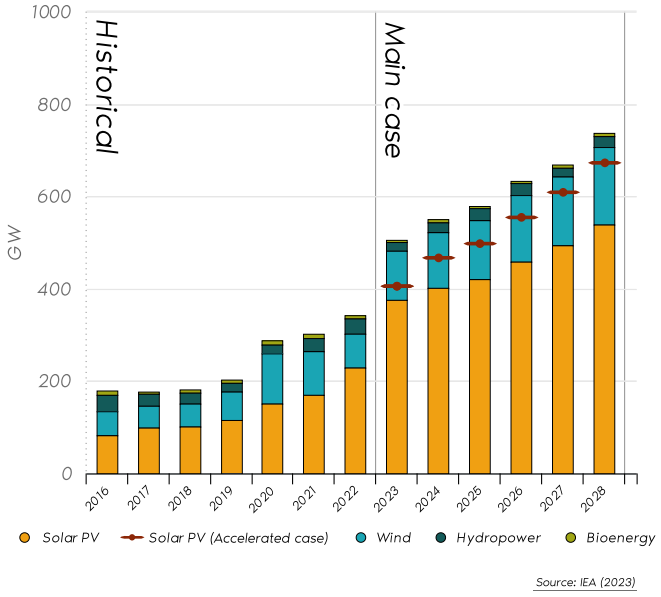


**Fig. 1.** Renewable electricity capacity additions by technology and segment, 2016–2028.

substantial absolute growth in generation among all renewable energy technologies but also surpassed wind power for the first time in history [6]. Solar PV and wind installations are projected to more than double by 2028 from the levels observed in 2022 (Fig. 1), consistently setting new benchmarks throughout the forecast period to approach a capacity of nearly 710 GW [6]. The advancement of PV technologies in decarbonizing the energy landscape is evident as PV has mitigated up to 720 million metric tons of CO2eq, based on the installed capacity by the conclusion of 2019. PV plays a crucial role in reducing global CO2 emissions, accounting for 1.7% or 2.2% of energy-related emissions and 5.3% of electricity-related emissions [7].

To accelerate the expansion of installed solar PV capacity and maximize its utilization, recommender systems play a crucial role identifying prosumers with higher prospects evaluating the compatibility of these energy sources with their comsumption habits and the feasibility of integrating PV energy sources on their buildings.

Recommender systems have emerged as valuable tools for guiding changes in building energy consumption decisions [8]– [11]. These systems, founded on algorithms and data analytics, provide personalized recommendations and strategies for optimizing energy use under energy efficiency or cost premises. By analyzing historical data, user preferences, and real-time inputs, recommender systems can inform flexible users of the options to minimize energy waste in specific appliances [9], reduce costs and improve comfort by changing habits in users [10] where the decisions made by flexible energy users are taken as reference and recommended to the more static ones. A common practice within these systems involves identifying clients who exhibit greater flexibility for potential participation in demand response initiatives or for undertaking actions through the utilization of load monitoring techniques. For instance, [10] categorizes users with high energy consumption levels and low costs as high DR users, while those with the opposite characteristics are classified as low DR users. This approach presents two drawbacks: the requirement to have knowledge of the end-users' costs (not any agent can do it) and a possible miss-classification as high DR of a commercial site with high consumption processes that are already set in low-price period, and they are not willing to change their behavior. According to [12], DR users have an easily predictable energy profile, with peaks indicating the periods during which DR activities can be implemented. However, peaks can be interpreted as the potential for manageable consumption if they do not occur consistently at the same time each day. A peak consumption pattern that consistently happens at the same time might not indicate a willingness to change its consumption behavior. Thus, the challenge is to determine with simple and explainable measures that an end-user has a high, consistent level and period-variable energy consumption. DR is a key element for the future sustainability of the electric system, several indicators are appearing about measuring the quality of the dispatch of the service [13,14], but there is a lack of DR indicators to determine which clients are suitable for these services by Distribution Sistem Operator (DSO), retailers or aggregators.

On the other hand, the topology of a building plays a critical role in assessing solar panel installation suitability. Traditionally, the

topological features considered in these studies are related to the building's area, tilt, orientation, and height [15]. These features determine the level of solar radiation expected. In particular, 3D building models are nowadays a reliable approach for studying how topological features play a critical role in the levels of solar exposure due to occlusions produced between buildings and surrounding elements and between structural elements of the same building. Simplified 3D geometric models are suitable for studying projected shadows between buildings, study of building density, etc. [16]. Still, when studying self-occlusions produced by smaller structural elements, these approaches require high-resolution 3D Models.

This research proposes two kinds of indicators whose objective is threefold: 1) Flexible consumption indicators, which detect flexible energy consumption patterns through explainable and straightforward methods to be able to be run in remote recommender systems without the need for databases; 2) Topology indicators, which score the suitability and eligibility of buildings' facades, roofs and structures for the installation of solar panels; 3) The aggregation of both indicators for cloud recommender systems, ease the decision-making process and interpretability for non-expert end-users. In addition, the first kind of indicators could be applied to tag the data used by the training stage of Machine Learning (ML) or Deep Learning (DL) based recommender systems. The second type assesses suitable areas for installing PV units as a percentage of the total property area and the level of radiation determined by the topological features and occlusion shades produced by surrounding and inner structures. Both sets of indicators are highly interesting for any agent (DSOs, generation companies, retailers, energy communities, end-users…) for energy usage improvements, studying their grids' flexibility, or exploring the potential benefits of installing local solar resources in a community. The paper starts with a literature review in section II and the definition of the new proposed indicators in section III. Section IV presents the datasets from REDREAM H2020 Project used to evaluate the indicators' results presented in Section V. Finally, Section VI concludes the key insights of the proposed set of indicators, their limitations and future works.

## 2. Literature review

The reviews [8,11] on these recommender systems analyze the future direction on this topic. Those authors highlight the importance of explainable systems that justify why these recommendations were triggered and their benefits. Other sustainability indicator approaches are based on ML techniques [17] like Random forest or Neural Networks such as Multi-Layer Perceptrons, presenting a limited interpretability of their parameters. Hence, the current primary focus is on explainability, as surveys [5] have indicated a lack of understanding among end users regarding smart grids and flexibility.

Research in recommender systems [8] is evolving toward using non-intrusive load monitoring (NILM) strategies and implementing this algorithm in the edge as a second novelty. NILM avoids sub-metering (cost-effective solutions) [18,19] and actions from users (installing equipment, sharing tariff…). This means that it could be used in the smart meter of the users or even in any meter within the grid owned by any agent that has access to power consumption time series data. However, most of them use different techniques (ML, DL, Hidden Markov Models) that require a huge amount of labeled data to classify and characterize devices and users' consumption habits. The execution of large dimensional models usually surpasses the limitations that embedded hardware devices present [19], unfollowing the second novel point in recommender systems.

Assessing the effectiveness and efficiency of the photovoltaic setup, considering consumption profiles and the topological features of support surfaces are critical factors [20,21] in determining suitability and feasibility for PV panel installation. Previous studies [22,23] assess the effectiveness of PV panels based on primary attributes such as tilt and orientation. The feasibility of a photovoltaic panel system is dependent not only on its tilt angle and orientation but also on the topological features of the support surface, available space, rooftop suitability, and the presence of surrounding structures that may have an impact on irradiance levels caused by shading effects and occlusions. [24] includes bare urban canopy features, spatial information, and building height estimations, which are especially relevant for assessing occlusions and shade projections on a large scale [25]. Approaches based on Digital Elevation Models [26], Hill shade analysis [27] or 3D building models obtained from Light Detection And Ranging images [15] and aerial orthographies [28] allow for substantial improvements in the characterization of topological features applied to the study of shadow projections and occlusions. [29] simulates solar radiation on buildings based on bare urban building geometries obtained from GIS data. [16,26] estimate solar radiation levels based on 2D building footprints / LiDAR images extruded manually as simplified 3D building blocks filtering out unwanted objects and including additional geographical information, elevation and irradiation seasonality features. [30] proposes a model to estimate building heights based on Satellite imagery, including a categorization of building rooftops. [31] proposes a 3D building information modeling (3D BIM) reconstructed using computer-aided design (CAD), including surrounding context information, especially relevant for studying irradiation on surfaces with singularities. Most of these researches have primarily focused on analyzing the irradiation performance of solar panels, with less emphasis on identifying suitable support areas. This focus point is attributed mainly to the requirement of high-resolution topological building models, often manually created, which poses a time-consuming challenge when conducting assessments on a large scale.

Studies like [28] show the complexity behind creating 3D building models at urban or neighborhood levels. Some open-source initiatives like osgEarth or OpenStreetMap provide mid-low resolution 3D models. Others, like Google Maps, provide, under commercial licenses, city-scale 3D models that include high-resolution topological features of any structure (not only buildings). Previous studies like [15,32] have already used 2D maps obtained from Google. In May 2023, Google announced the experimental release of Photorealistic 3D tiles. One of the novelties of this study relies on this cutting-edge technology based on high-resolution 3D maps (tiles), allowing for a substantial improvement in the detection of unfeasible areas and characterization of topological features for the installation of solar panels. Studying light projections and shades in buildings with a complex topology becomes an easy task for 3D computer graphics tools already tested in applications like Solar3D [33] or Blender [34,35]. Blender outperforms the film and animation industries, simplifying the simulation of the light behavior (radiation) represented as a rendered scene.

## 3. Creation of indicators for recommended systems

### 3.1. Flexible consumption indicators

Extensive research has been conducted on the limitations of existing tools for classifying flexible clients, highlighting the importance of indicators that are easy to comprehend, explainable, and computable on remote devices. For those reasons, fundamental statistical indicators are utilized to create additional indicators to identify consistent energy patterns that are easily predictable but exhibit variability in power consumption. In particular, the indicators comprise three main categories:

- Consumption level: The amount of energy demanded by a consumer. A higher energy consumption level could mean more energy to be offered in markets. This concept can be translated as the greater the energy that an individual user can shift, the less necessity there is to

[1] In order of appearance in the appendix

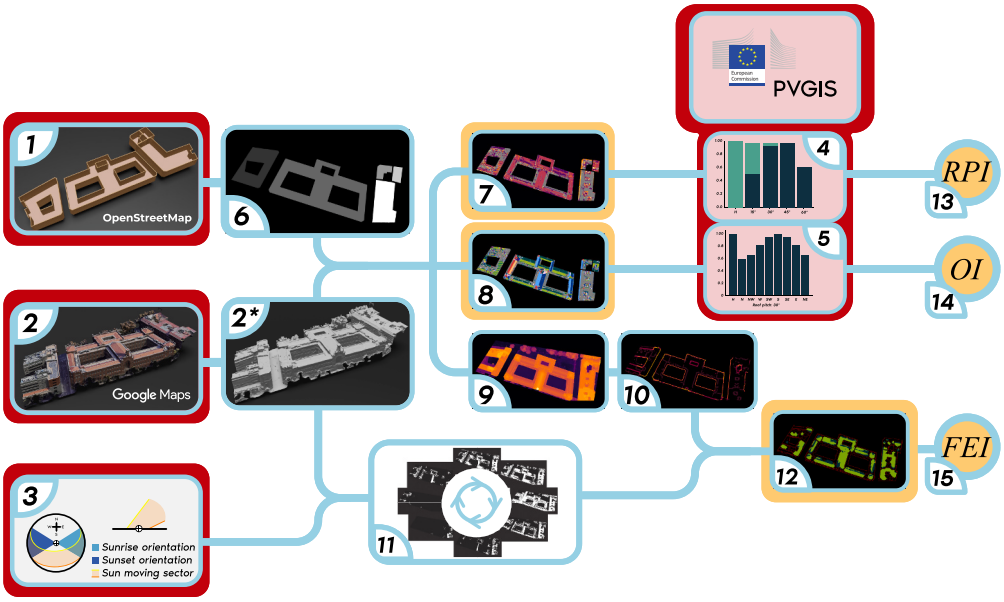


**Fig. 2.** Workflow for the composition of topology indicators.

aggregate multiple users. The Energy Level Indicator (ELI) grades the daily energy consumption by different levels.

- Consumption consistency: These indicators determine the stability of the energy usage: if the user is stable in their energy consumption habits, the amount of energy is stationary and easy to predict. These results could represent the confidence level that this user offers to their DR manager. Individuals with unpredictable energy consumption profiles and erratic consumption patterns pose an increased risk when being evaluated for participation in explicit DR bids within markets. Two indicators are considered to measure consistency: the Energy Consistency Indicator (ECI) measures the consistency of consumption profiles in all hours among days, and the Energy Variation Indicator (EVI) assesses the consistency of total energy consumption across different days.
- Consumption variability: This category aims to determine the potential for load-shifting in users' consumption patterns without needing equipment data or intrusive local monitoring. This approach involves analyzing the power fluctuations in each hour of the day by examining the interquartile range or its standard deviation to determine the Amplitude Level Indicator (ALI) or the Standard Deviation Indicator (SDI), respectively.

The six indicators introduced here are presented individually in the appendix:

1) Energy Level of Consumption (ELI)

The first and most straightforward indicator, formulated by algorithm 1 in the appendix, for assessing energy usage is the daily mean energy consumption, as clients with higher consumption levels are likely to be more interested in participating than those with lower consumption profiles. The algorithm should be normalized or levelized when considering a reduced set of hours to ensure fair comparison and accurate analysis. This adjustment can be made by choosing an appropriate value for H as a maximum energy reference (e.g., twice the average household consumption level) and L as a low energy level resulting from minimal consumption. A final remark is that users with higher energy consumption levels are generally more suitable candidates for installing PV panels, as they can benefit more from solar energy's potential savings and environmental impact.

2) Energy Consistency per period (ECI)

This indicator assesses the stability and daily variations of end-user energy consumption and is formulated in algorithm 2 in the appendix. This indicator was previously presented in [12] to score the predictability of the baseline consumption of users based on the mean, M, and the standard deviation, S, of the power demand in each interval. While it is reasonable to rely on a predictable baseline, the limitation of this assumption is that users with consumption patterns unrelated to habits, who may consume energy at any time of day, such as processes that require a specific number of operating hours per day, can be penalized when only this indicator is considered.

3) Energy Level Variation of consumption (EVI)

This indicator characterizes the consistency of energy usage as the standard deviation coefficient of the daily energy demand, and it is formulated in algorithm 3 in the appendix. Users are more flexible resilient if their total level of energy consumption does not vary among days. Thus, a low standard deviation, S, is a desired output. The difference with the previous indicator is that users whose consumption is produced at different hours are not penalized. The suggested values here are relative to the mean, M, of the daily consumptions based on their coefficient of variation $S/M < 0.1$.

4) Interquartile Power Range (ALI)

This indicator is the first (from the list of indicators proposed so far) to measure the power variability, and it is formulated in algorithm 3 in the appendix. It uses the first and third quartiles to identify the interquartile range of the changes, robustly mitigating the impact of outliers in the power time series to establish different levels. This indicator is evaluated in different time windows to remove the bias of those periodic consumptions that take place at the same time each day. The reference of a high amplitude level, H, can be set according to power of appliances or based on the minimum bid size needed by the DR manager. This value is based on expert criteria.

5) Power Standard Deviation (SDI)

The second indicator to measure deviations in consumption profiles

is based on traditional statistical measures of the standard deviation. This can be used to establish levels of power that are considered to be the minimum variation. In the same way, the indicator considers multiple time windows to remove the scheduled consumptions. The highest reference value, H, is related to the high value in the previous indicator. For instance, since 95% of data are within two times the standard deviation of the whole timeseries, the reference value used in algorithm 4 could be divided by two to obtain a possible H value for this algorithm.

6) Flexible Consumption Indicator

The most suitable approach for aggregating all the indicators mentioned earlier depends on expert criteria. Among the possible aggregating methods, the most common ones are arithmetic and geometrical [36]. The main difference is that arithmetic aggregation allows for compensations between values, while geometrical does not allow for any compensation between indicators with disparate values (fungibility issue). Since some of them could be zero, an arithmetic average is proposed with indicators 2–3 for consistency and the same with indicators 4–5 for variation. Then, a geometric mean is computed (See Eq. (1)), including the energy level indicator. All indicators must have the same temporal framework (working hours, weekends…).

$$Total\ (I_1) = ELI^{1/3}\cdot(ECI\cdot 0,5 + EVI\cdot 0,5)^{1/3}\cdot(ALI\cdot 0,5 + SDI\cdot 0,5)^{1/3} \quad (1)$$

### 3.2. Topology indicators

The topology of a building is a critical aspect to be assessed and studied when it comes to considering the installation of solar panels on rooftops and facades. The composition of these indicators follows the workflow presented in Fig. 2.

The workflow starts with five inputs:

1) Boundaries of property/buildings. This layer is obtained from OpenStreetMap. This layer allows for the segmentation of buildings, which is crucial for identifying connected structures that cannot be visually separated. In case that small variations in terms of scale and location of each building when it comes to merging it with input layer 2), this layer has to be manually aligned.
2) High-resolution 3D building models. This layer is obtained from Google Maps, and it is the most critical layer. It contains high-resolution topological features related to pitch angle, orientation, height, discontinuities in the surface, etc.

2*) High-resolution 3D building models without surface texture.

3) Sunrise, sunset and sun movement parameters. These parameters allow for the 4D simulation (3D + time) of the sun paths in Blender. These parameters depend on the region's location and season.
4) Radiation levels depending on the roof pitch angle. Radiation levels based on the pitch angle are obtained from the Photovoltaic Geographical Information System (PVGIS) [37]. Those values are computed for a costant orientation (South for northern hemisphere regions and North for southern hemisphere regions) and normalized [0.5–1] based on the maximum radiation according to Eq. (2):

$$R_{pitch}{}' = 0.5 + 0.5\cdot\frac{R_{pitch} - R_{\min}}{R_{\max} - R_{\min}} \quad (2)$$

where $R_{pitch}{}'$ is the normalized radiation value, $R_{\min}$and $R_{\max}$are the minimum and maximum radiations registered, respectively. In cases where the steeper the pitch, the higher the radiation, its value is assigned to the maximum radiation achieved with a steeper pitch. Flat (horizontal) surfaces are considered the "best possible" slope, allowing for any slope configuration for the PV modules.

Normalized radiation levels depending on roof pitch angles for a constant roof orientation (South) obtained from PVGIS in a specific location (Bath, United Kingdom) are shown in Fig. 3.

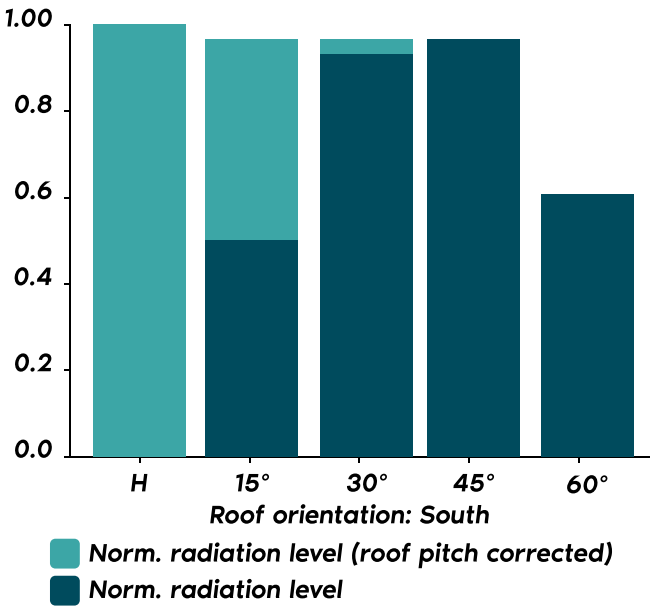


**Fig. 3.** Normalized radiation levels depending on the roof pitch angle for a constant orientation (South).

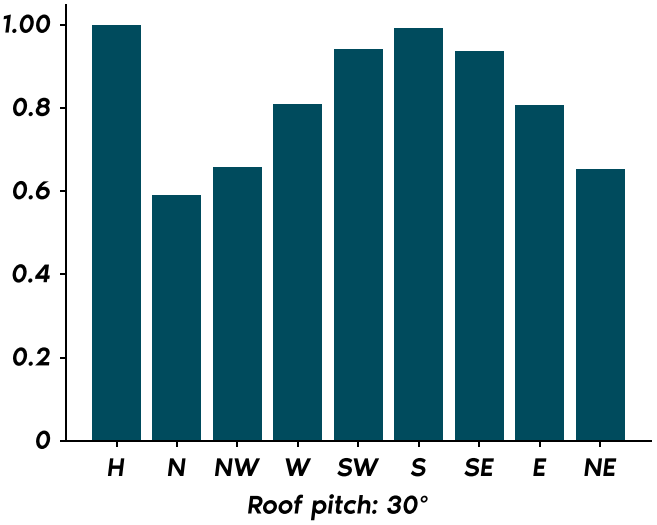


**Fig. 4.** Normalized radiation levels depending on the roof orientation for a constant pitch angle of 30°.

5) Radiation levels depending on the orientation of the supporting structure. These values are also obtained from PVGIS. Radiation values are computed for slope values fixed to 30° and normalized to 1 using the maximum radiation level register among all orientations according to Eq. (3).

$$R_{orientation}{}' = \frac{R_{orientation}}{R_{\max}} \quad (3)$$

Normalized radiation levels depending on the roof orientation for a constant pitch angle of 30° obtained from PVGIS in a specific location (Bath, United Kingdom) are shown in Fig. 4. Again, horizontal surfaces are deemed the optimal orientation, permitting PV modules to be

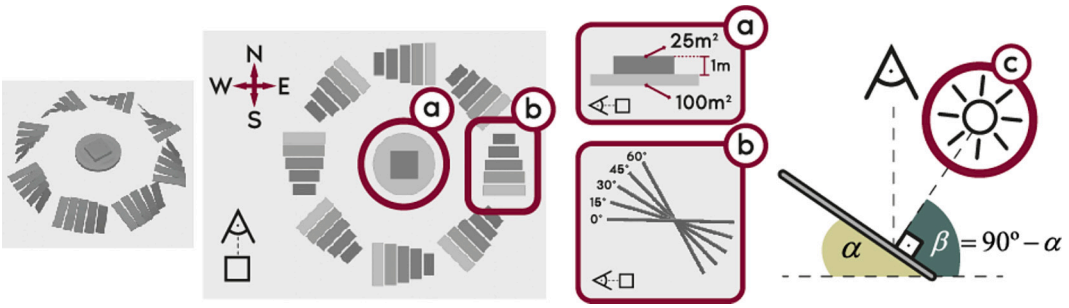


**Fig. 5.** 3D Benchmark used to validate the identification of orientation and pitch angles of surfaces.

installed in any orientation.

The second stage focuses on identifying topological features and rendering them into layers. Layers are matrix information that can be visualized as images. In this stage, the following layers are computed:

6) ID layer. Based on the boundaries of each building, each property is tagged with a unique ID.
7) Orientation layer. Lighting the 3D model with different orientations, it is possible to identify the direction in which the surface becomes more enlightened.
8) Roof pitch layer. It is possible to determine the pitch of a surface as the angle at which the surface receives more light by illuminating the 3D model at different angles or by through the slope of normal vector of the surfaces of the building model.
9) Elevation layer. The elevation of the 3D model is rendered as an OpenEXR image with values between 0 and 1 assigned to the lowest and highest points, respectively. This image format allows for a high dynamic range to render the height values of the 3D model, preserving original shapes and proportions.
10) Discontinuities layer. Based on the elevation layer, it is possible to identify surface discontinuities. Discontinuities represent sharp variations (>1 m) in the height of a surface, which can hinder or even impede the installation of PV modules. Small regions surrounded by discontinuities and regions next to discontinuities are considered unsuitable for installing PV modules. Discontinuities are obtained as the maximum absolute value of the convolution products using four kernels, one per direction. The kernels used are shown in (4):

$$\begin{pmatrix} 0 & 1 & 0 \\ 0 & 0 & 0 \\ 0 & -1 & 0 \end{pmatrix}, \begin{pmatrix} 0 & 0 & 0 \\ 1 & 0 & -1 \\ 0 & 0 & 0 \end{pmatrix}, \begin{pmatrix} 1 & 0 & 0 \\ 0 & 0 & 0 \\ 0 & 0 & -1 \end{pmatrix}, \begin{pmatrix} 0 & 0 & 1 \\ 0 & 0 & 0 \\ -1 & 0 & 0 \end{pmatrix} \tag{4}$$

A 3D benchmark is attached to the 3D model in order to test the robustness of this approach. This 3D benchmark allows for identifying the angle and orientation of the surfaces enlightened from nine orientations [Vertical, West, South-West, South, South-East, East, North-East, North, North-Weast] and five angles [0°, 15°, 30°, 45°, 60°]. The 3D benchmark elements are shown in Fig. 5.

The elements that make up the 3D benchmark are:

a) Size of reference. The 3D benchmark is upscaled until its central area is equal to 100m$^2$ (according to the scale of the 3D model). On top of the circular area, an additional squared area of 25m$^2$ and 1 m height is added. The benchmark scale is based on the proportions of two measures, one in Blender and another in Google Maps. This benchmark allows for measuring areas (in pixels) and discontinuities (vertical variations between surfaces).

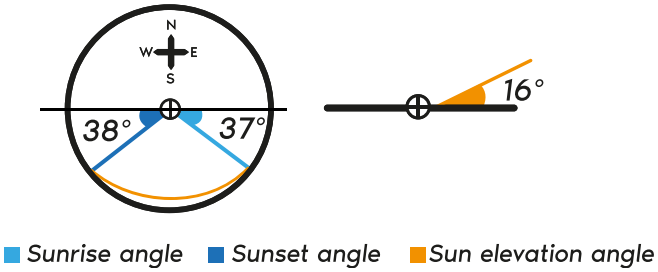


**Fig. 6.** Configuration used to simulate the sun trajectory.

b) Reference orientation and pitch module. Eight modules with five pitched tiles each, one for each angle (40 tiles in total) are attached around the central area, allowing for measuring the orientation and pitch of surfaces.
c) Artificial light. Surfaces are enlightened with a moving light faced toward each orientation and pitch angle (33 light positions in total). The maximum reflected light is produced when the artificial light is perpendicular to the surface. The elevation of the light ($\beta$) corresponds to the complementary angle of the pitched tile ($\alpha$).

Orientation and pitch angles can be obtained programmatically from the 3D mesh rasterizing as an image the normal vector of each face of the 3D mesh. As the lighting method can be easily reproduced in any 3D graphics software, this method was eventually chosen for this purpose.

The third stage comprises the lighting simulation (sun path) and discontinuity assessment. The layers generated in this stage are:

11) Solar lighting (sun path) sequence. This set of layers includes the simulation of shades and occlusions produced during the movement of the sun throughout a single day. Sunrise, sunset and maximum elevation angles are determined as the mean values of maximum and minimum values registered in a specific location throughout a year. The sequence is made up of 52 snapshots, where first and last snapshots are sunrise and sunset conditions. Low exposure areas are those that are enlightened less or equal to 50% of the snapshots. On the contrary, high-exposure areas are those that are enlightened by >50% of the snapshots. The parameters to simulate the sun trajectory in Blender correspond to winter trajectories where the angle between sunrise and sunset and the elevation are the smallest (most restrictive conditions) as shown in Fig. 6.

12) Feasible exposure levels layer. Combining the results obtained from the solar lighting sequence and discontinuity layer allows for identifying which surfaces are more suitable for installing PV modules due to their high exposure level and lack of discontinuities. This layer is the most critical among the three output layers (7, 8, and 12) as it determines the total surface that can be used for installing PV modules. Areas adjacent to or surrounded

**Table I**
Comparison to previous studies for the assessment of topological features of buildings.

| | [24] | [25] | [16] | [30] | [29] | [31] | This study | Indicator |
|---|---|---|---|---|---|---|---|---|
| Area + Height | ✔ | ✔ | ✔ | ✔ | ✔ | ✔ | ✔ | |
| Rooftop discontinuities | | | | | | | ✔ | |
| Non-structural surrounding context (e.g. trees…) | | | | | | | ✔ | FEI |
| Building + rooftop orientation (coarse) | ✔ | ✔ | ✔ | ✔ | ✔ | ✔ | ✔ | |
| Rooftop orientation (detailed) | | | | | | ✔ | ✔ | OI |
| Rooftop type (coarse features) | | | | ✔ | ✔ | ✔ | ✔ | |
| Rooftop pitch angle | | | | | | ✔ | ✔ | RPI |
| Large scale building models | ✔ | ✔ | | ✔ | ✔ | | ✔ | |

by discontinuities are classified as unsuitable areas. Unsuitable areas are determined through morphological transformations such as dilation, erosion, openings, and closings applied to the identified discontinuities.

Three indicators are computed for each building using the information obtained from layers 7, 8, and 12:

13) Roof pitch indicator. Computed in a similar way to the previous one as shown in Eq. (5):

$$RPI = \frac{\sum_i N_i \cdot R_i}{N_{total} \cdot R_{max}} \quad i \in [0^\circ, 15^\circ, 30^\circ, 45^\circ, 60^\circ] \tag{5}$$

Where $N_i$ is the number of pixels of a structure with a pitch $i$, $R_i$ is the normalized radiation level corresponding to pitch $i$, $N_{total}$ is the total number of pixels of the structure, and $R_{max}$ is the best possible normalized radiation level ($R_{max}$= 1) for the best pitch angle with a south orientation.

14) Orientation indicator. Computed as depicted in Eq. (6):

$$OI = \frac{\sum_i N_i \cdot R_i}{N_{total} \cdot R_{max}} \quad i \in [V, W, SW, S, SE, E, NE, N, NW] \tag{6}$$

Where $N_i$ is the number of pixels with an orientation $i$, $R_i$ is the normalized radiation level corresponding to orientation $i$, $N_{total}$ is the total number of pixels of the structure, and $R_{max}$ is the best possible normalized radiation level ($R_{max}$= 1) for the best orientation, with a pitch fixed to 30°.

15) Feasible exposure indicator. This indicator quantifies the number of pixels that belong to feasible areas with a high exposure relative to the total number of pixels of the structure. It is computed as shown in Eq. (7).

$$FEI = \frac{N_i}{N_{total}} \tag{7}$$

Where $N_i$ is the number of pixels of suitable areas with high exposure levels and $N_{total}$ is the total number of pixels of the structure.

The last stage aggregates the three indicators obtained into a single composite indicator. As it was done with the flexible indicators, a composite indicator regarding the topological features is computed as shown in Eq. (8):

$$Total\ (I_2) = RPI^{0.15} \cdot OI^{0.15} \cdot FEI^{0.7} \tag{8}$$

Where $I_2$ is the final score regarding to the topological features, RPI is the score for the pitch, OI for the orientation, and FEI for the exposure level. Their weights (based on expert criteria) are 0.15, 0.15, and 0.7, respectively.

This study stands out from previous studies on analyzing solar radiation levels and feasible surfaces in 3D building models by being the first to assess detailed large-scale building models, including an exhaustive rooftop characterization and non-structural surrounding context. A set of detailed topological features allows for the estimation of expected radiation levels on rooftops as well as a comprehensive assessment of the available space for the installation of sustainable energy sources. This last aspect was not included in any of the previous studies but in this one (See Table I).

Non-structural surrounding context is crucial for the identification of high exposure regions when the building is surrounded by higher elements, an example of this situation is shown in Fig. 7 where a set of adjacent trees projects shades over the rooftop of houses located nearby.


**Fig. 7.** Example of occlusions produced by non-structural surrounding elements of higher dimension.

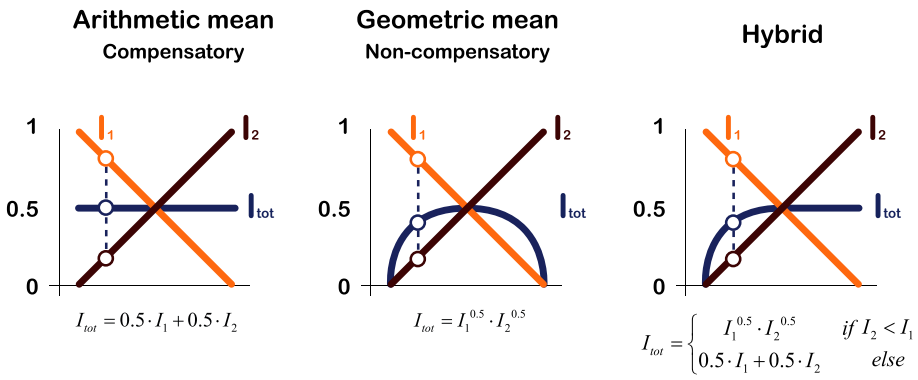


**Fig. 8.** Aggregation methods considered for the composition of the final indicator.

**Table II**
User characteristics.

| ID | 1 | 2 | 3 | 4 | 5 | 6 | 7 | 8 | 9 | 10 | 11 | 12 |
|---|---|---|---|---|---|---|---|---|---|---|---|---|
| Location | SP | SP | IT | UK | UK | IT | SP | HR | UK | UK | HR | SP |
| Type | Residential | Residential | Residential | Residential | Residential | Public Building | Office | Residential | Residential | Residential | Residential | Office |

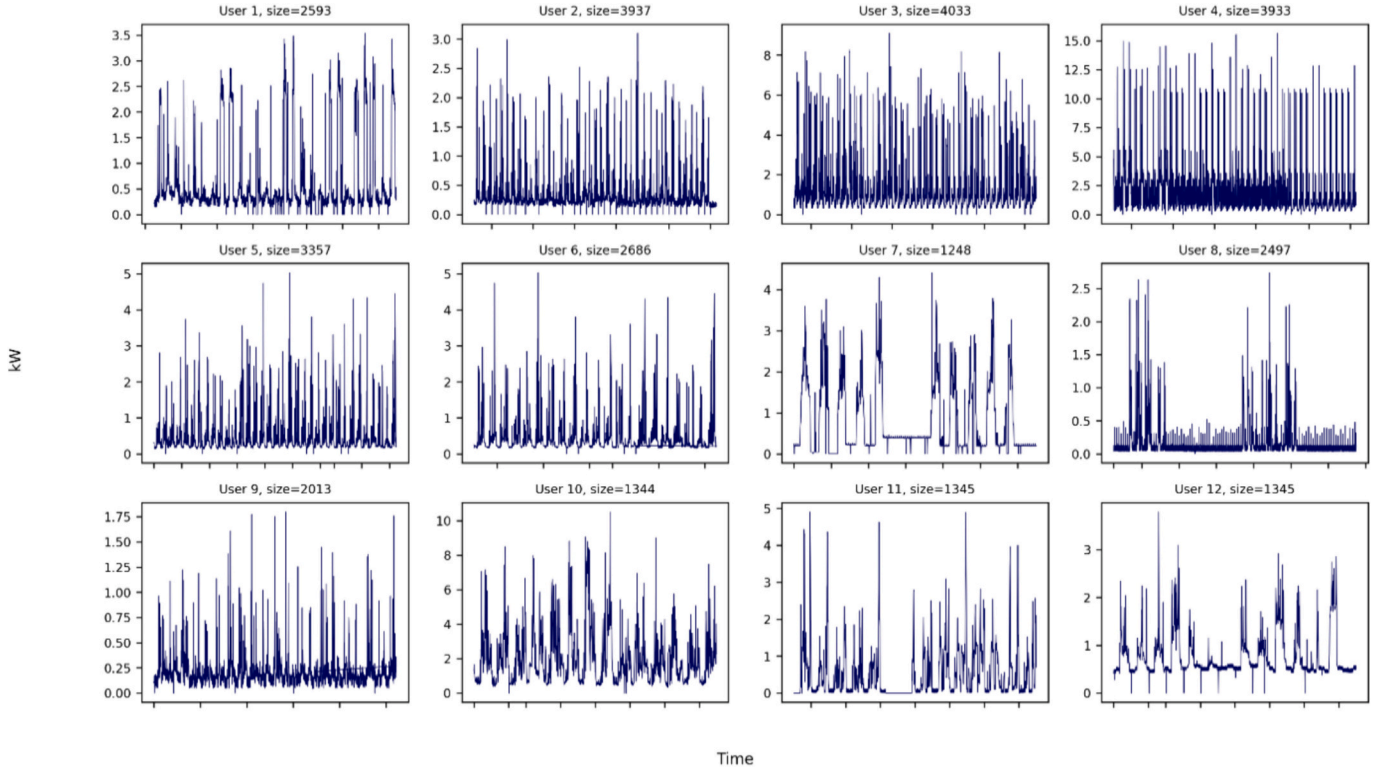


**Fig. 9.** *Power consumption Timeseries* [42].

### 3.3. Aggregation of flexible and topology indicators

The last step of this methodology is aggregating the total indicator for flexible consumption ($I_1$) and topology indicators ($I_2$). Again, arithmetic and geometric aggregations are considered [36]. The main difference between arithmetic (compensatory) and geometric (non-compensatory) aggregations is that compensatory aggregation combines multiple attributes using a weighted average, allowing for trade-offs between variables. In contrast, non-compensatory aggregation uses a minimum or maximum threshold approach, where both indicators must be higher than a specific value. Compensatory effects of the three approaches considered (arithmetic, geometric, and hybrid) are depicted in Fig. 8.

Recent studies in composite indicators [38–40] only consider one type of aggregation (geometric or arithmetic). For this study, standard aggregation methods present limitations. It must be noted that the Topology index does not allow any type of compensation, whereas the Flexible Consumption index is convenient but not crucial to a certain extent.

This assumption requires a hybrid aggregation where compensations

**Table III**
Temporal aggregation for the flexible indicator cases.

| Aggregation | Full Week | Sun | No Sun | Work | After Work | LV | SD |
|---|---|---|---|---|---|---|---|
| Days | L-D | L-D ago-19 | L-D | L-V sep-18 | L-V | L-V | S-D |
| Hours | 0–23 | | 0–7,20–23 | | 18–24 | 0–23 | 0–23 |

are only considered in those cases where the Topology Indicator ($I_2$) is greater than the Flexible indicator ($I_1$). Fig. 11 and Table *VI* show the results obtained through a hybrid aggregation of both indexes equally weighted according to Eq. (9):

$$I_{tot} = \begin{cases} {I_1}^{0.5} \cdot {I_2}^{0.5} & if\ I_2 < I_1 \\ 0.5 \cdot I_1 + 0.5 \cdot I_2 & else \end{cases} \quad (9)$$

## 4. Datasets and cases

Solar and consumption data from the H2020 REDREAM project [41] will be used to test the indicators proposed. REDREAM project enables flexible consumers and prosumers to participate in the energy market. REDREAM has four demo locations: Bath (UK), Valladolid (Spain), Gallese (Italy) and Varazdin (Croatia).

Table II shows the location, type, size and number of usual inhabitants in some of the most active buildings from the project. The consumption curves of each of the users are shown in Fig. 9. Different lengths of curves can be seen due to the difference in the installation date of the smart meters that offer energy information each 15 min. Data collection starts on May 29 in cases where it is available [42]. Different energy levels can also be observed, being the power level calculated from each 15-min energy measurement sample.

In order to test the flexibility indicators and their relationship with the solar indicator to make comprehensive recommendations, different time aggregations have been considered (Table III). First, the indicator is analyzed during solar hours to determine if the consumption is manageable during those periods. Second, since most of the users are residential or office, knowing if the users are more flexible in working or after work periods during working days can offer interesting results for cases where the type is unknown. Finally, a differentiation between working days and weekends is conducted.

The portfolio of users is quite heterogeneous in terms of energy level usage. A high daily energy level of 20 kWh was chosen and adjusted based on the number of aggregation hours. The low energy level was established as 10% of the high level for algorithm 1. The confidence level for the algorithm is set in two standard deviations. The high level, H, of amplitude and standard deviation for residential and commercial levels have been set at 1.5 kW and 0.75 kW, respectively. As proof of concept for the topology indicators, twelve buildings with characteristics similar to those used in the flexible indicators were selected from Bath, England.

## 5. Results

### 5.1. Flexible consumption indicators

The case study presented involves twelve anonymized end users from the REDREAM project. Each time series has different dates since each client starts on a different day, but all of them have more than a week of power consumption data in intervals of 15 min to perform this analysis.

Results of the indicators show the importance of the temporal aggregations since each client shows a higher score in different aggregations (Fig. 10). The total indicator ($I_1$) is used to measure the final score of each user, although showing each indicator manifests the benefits of using different measures.

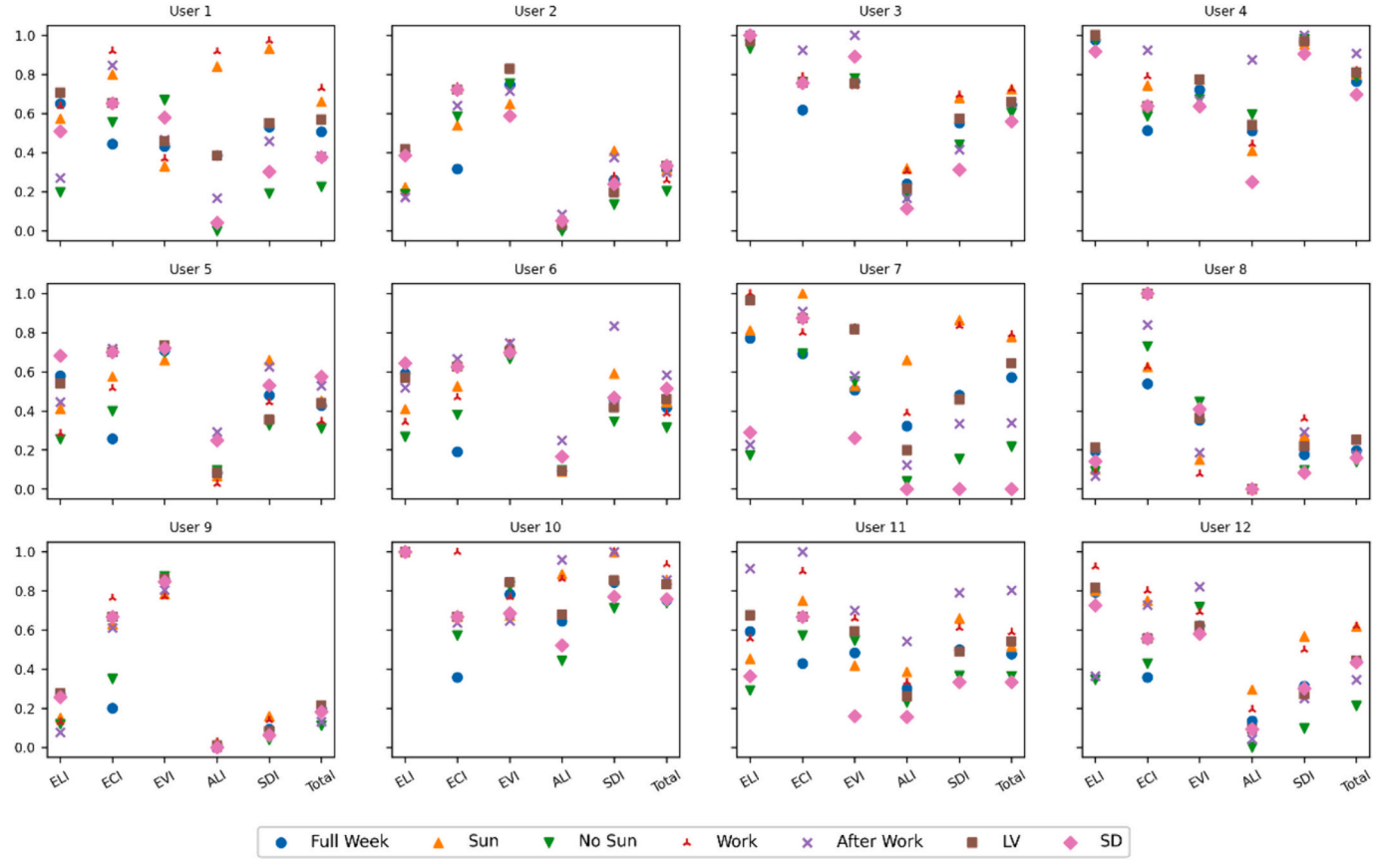


**Fig. 10.** Scores for different time aggregations.

**Table IV**
Comparison to previous studies in the field of Flexible Consumption Indicators.

| Ref | Methodology/ Indicator used | Advantages of the proposed indicators |
|---|---|---|
| [9] | Probability-Density-Function | Probability Density-Functions are based on the rest of population actions, in this case it would need a previous portfolio of flexible clients. In our approach, obtain the indicator to make the recommendation for installing solar or DR opportunities is not portfolio dependent. |
| [10] | ELI | Our set of indicators enhanced reliability in identifying flexible clients beyond just larger clients. Only User 7 and 12 that are offices would have been classified as flexible, missing 4 or 10, for instance. The use of the proposed indicators improves the identification of flexible consumptions in a wider range of users. |
| [12] | ECI | Even in the same category of consistency ECI and EVI indicators depict different results in all users. A single indicator (ECI) is not enough to categorize flexible users. User 8 would be a clear example of misclassification. |
| [17] | ML/DL | The methods suggested in the prior study are not suitable for edge deployment and require a large amount of data to start operating. In addition, those methods are black boxes. Our methodology has been tested with real clients with only a week of data. |

For instance, users 7 and 12, which are offices, present higher scores in work and sunny hours and working days. This fact is logical in the case of offices, but some residential users also present these characteristics as users 1, 10. In particular, user 1 is a curious case of residential users since it consumes less during afterwork hours than during working hours. This fact makes this user, who could be a retired person or remote worker, candidate for solar panels since their flexible consumption matches those hours, meaning there is potential to adapt their consumption to solar generation.

On the other hand, there are users that their flexibility increases in afterwork hours. Here, a distinction can be seen since some of them also score high on weekends (5,6). Users 3, 4, and 11, who do not have high scores on weekends, may be individuals who spend their weekends in a second residence or engage in outdoor activities. The regional context seems irrelevant in this case since users from different countries made each of these groups. Depending on their energy consumption level, those users could be interested in storage systems in combination with solar panels. The rest of the users (2,8,9) exhibit low variation indicator scores. Despite some aggregations showing energy consistency usage patterns, their low-level energy consumption leads to final scores below 40% for all of them.

It is crucial to consider the different indicators in order to gain a comprehensive understanding of the situation. Relying solely on ELI may lead to overlooking significant insights and information. For instance, user 10 has high energy consumption levels independently of the time aggregation, but other indicators can differ that working days from 8 h–24 h have higher flexibility than the rest of the hours. In fact,

**Table V**
Results obtained for the topological indicator corresponding to the set of chosen buildings.

| A | | Residential | | Residential | | Residential | | Residential | | Residential | | Public Building | | Office | | Residential | | Residential | | Residential | | Residential | | Office | |
|---|---|---|---|---|---|---|---|---|---|---|---|---|---|---|---|---|---|---|---|---|---|---|---|---|---|
| B | |  | |  | |  | |  | |  | |  | |  | |  | |  | |  | |  | |  | |
| C | |  | |  | |  | |  | |  | |  | |  | |  | |  | |  | |  | |  | |
| D | | 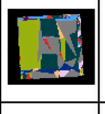 | |  | |  | |  | | 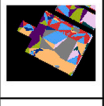 | | 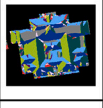 | |  | |  | |  | | 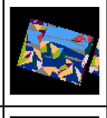 | |  | | 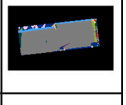 | |
| E | |  | |  | | 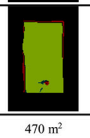 | |  | |  | |  | |  | |  | |  | |  | |  | |  | |
| F | | 260 m² | | 400 m² | | 470 m² | | 70 m² | | 290 m² | | 1800 m² | | 1260 m² | | 115 m² | | 820 m² | | 220 m² | | 215 m² | | 530 m² | |
| * C | 0°: 1.0 | 0.29 | 0.95 | 0.18 | 0.97 | 0.93 | 0.99 | 0.24 | 0.96 | 0.18 | 0.95 | 0.14 | 0.95 | 0.14 | 0.93 | 0.02 | 0.94 | 0.1 | 0.9 | 0.11 | 0.95 | 0.16 | 0.97 | 0.79 | 0.97 |
| | 15°:0.97 | 0.23 | | 0.02 | | 0.03 | | 0.06 | | 0.16 | | 0.32 | | 0.16 | | 0.15 | | 0.13 | | 0.13 | | 0.05 | | 0.07 | |
| | 30°:0.97 | 0.24 | | 0.79 | | 0.01 | | 0.29 | | 0.06 | | 0.33 | | 0.43 | | 0.49 | | 0.13 | | 0.41 | | 0.39 | | 0.03 | |
| | 45°:0.97 | 0.18 | | 0.02 | | 0 | | 0.39 | | 0.55 | | 0.14 | | 0.17 | | 0.27 | | 0.44 | | 0.3 | | 0.38 | | 0.04 | |
| | 60°:0.6 | 0.06 | | 0 | | 0.02 | | 0.03 | | 0.05 | | 0.06 | | 0.11 | | 0.07 | | 0.2 | | 0.05 | | 0.01 | | 0.06 | |
| * D | H: 1.0 | 0.29 | 0.84 | 0.18 | 0.83 | 0.93 | 0.99 | 0.24 | 0.89 | 0.03 | 0.86 | 0.14 | 0.82 | 0.14 | 0.81 | 0.02 | 0.82 | 0.1 | 0.82 | 0.11 | 0.84 | 0.16 | 0.83 | 0.79 | 0.97 |
| | N:0.59 | 0.04 | | 0.03 | | 0.02 | | 0.06 | | 0.1 | | 0.19 | | 0.3 | | 0.22 | | 0.06 | | 0.23 | | 0.02 | | 0.06 | |
| | NW:0.66 | 0.01 | | 0.01 | | 0.01 | | 0.02 | | 0.12 | | 0.02 | | 0.02 | | 0.12 | | 0.22 | | 0.06 | | 0.19 | | 0.0 | |
| | W:0.81 | 0.28 | | 0.0 | | 0.02 | | 0.25 | | 0.22 | | 0.18 | | 0.02 | | 0.24 | | 0.06 | | 0.08 | | 0.01 | | 0.02 | |
| | SW:0.94 | 0.02 | | 0.4 | | 0.01 | | 0.03 | | 0.08 | | 0.02 | | 0.03 | | 0.14 | | 0.13 | | 0.13 | | 0.22 | | 0.01 | |
| | S:0.99 | 0.04 | | 0.0 | | 0.0 | | 0.34 | | 0.08 | | 0.21 | | 0.36 | | 0.18 | | 0.06 | | 0.23 | | 0.03 | | 0.06 | |
| | SE:0.93 | 0.03 | | 0.0 | | 0.01 | | 0.0 | | 0.14 | | 0.03 | | 0.04 | | 0.01 | | 0.21 | | 0.05 | | 0.17 | | 0.02 | |
| | E:0.81 | 0.25 | | 0.0 | | 0.01 | | 0.06 | | 0.18 | | 0.19 | | 0.05 | | 0.05 | | 0.05 | | 0.08 | | 0.02 | | 0.03 | |
| | NE:0.65 | 0.03 | | 0.38 | | 0.0 | | 0.0 | | 0.05 | | 0.02 | | 0.03 | | 0.04 | | 0.1 | | 0.03 | | 0.17 | | 0.01 | |
| * E | LOW: | 0.44 | 0.56 | 0.27 | 0.73 | 0.03 | 0.97 | .21 | 0.79 | 0.37 | 0.63 | 0.45 | 0.55 | 0.68 | 0.32 | 0.55 | 0.45 | 0.73 | 0.27 | 0.5 | 0.5 | 0.41 | 0.59 | 0.03 | 0.97 |
| | HIGH: | 0.56 | | 0.73 | | 0.97 | | 0.79 | | 0.63 | | 0.55 | | 0.32 | | 0.45 | | 0.27 | | 0.5 | | 0.59 | | 0.97 | |
| TOTAL ($I_2$) | | 0.65 | | 0.78 | | 0.98 | | 0.83 | | 0.7 | | 0.63 | | 0.43 | | 0.56 | | 0.38 | | 0.6 | | 0.67 | | 0.97 | |

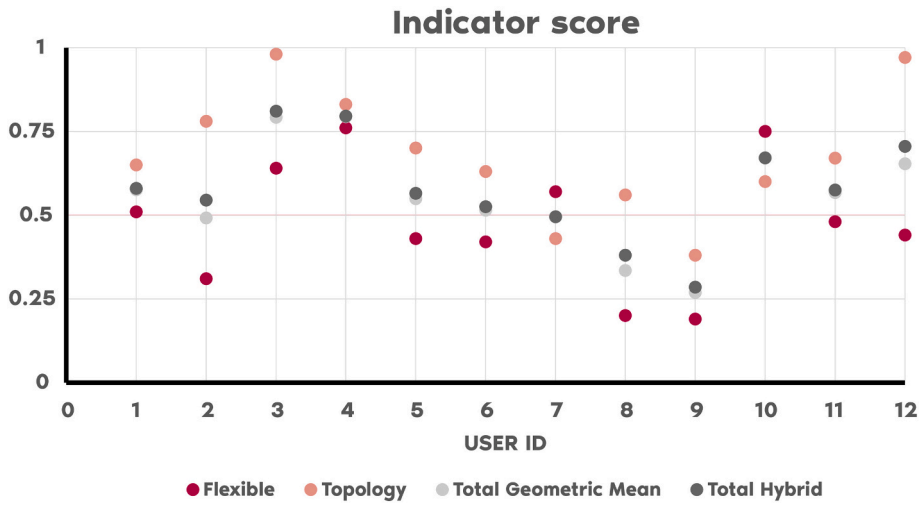


**Fig. 11.** Comparison of the Total Score using a geometric mean and a hybrid approach.

**Table VI**
Indicator Scores.

| ID | Flexible $I_1$ | Topology $I_2$ | Total Geometric $I_{TOT}$ | Total Hybrid $I_{TOT}$ |
|---|---|---|---|---|
| 1 | 0.51 | 0.65 | 0.58 | 0.58 |
| 2 | 0.31 | 0.78 | 0.49 | 0.55 |
| 3 | 0.64 | 0.98 | 0.79 | 0.81 |
| 4 | 0.76 | 0.83 | 0.79 | 0.8 |
| 5 | 0.43 | 0.7 | 0.55 | 0.57 |
| 6 | 0.42 | 0.63 | 0.51 | 0.53 |
| 7 | 0.57 | 0.43 | 0.5 | 0.5 |
| 8 | 0.2 | 0.56 | 0.33 | 0.38 |
| 9 | 0.19 | 0.38 | 0.27 | 0.29 |
| 10 | 0.75 | 0.6 | 0.67 | 0.67 |
| 11 | 0.48 | 0.67 | 0.57 | 0.58 |
| 12 | 0.44 | 0.97 | 0.65 | 0.71 |

considering other indicators improves the detection of the moments of greater flexibility. This can be seen in the change of ranking order of the time aggregations, comparing ELI with Total, in users 1,3,4,5,6,7,8,11 and 12. In the same way, ECI can have a higher value showing a very static behavior as in the case of user 8. In the case of.

user 8, a valid indicator could be the EVI that is low because has high volatility in their energy usage. However, this is not valid in user 9 where the level of energy usage is constant but the ELI and variations (ALI and SDI) are quite low. The SDI indicator always has higher values than the ALI indicator and sometimes the ranking order of the temporal aggrupation changes as observed in users 2 or 5.

Main advantages compared with existing literature are shown in Table IV.

### 5.2. Topology indicators

Although the results were computed for >1500 buildings [42], only twelve are shown in Table V. The results shown in this table are: A) Building type*; B) Aerial image of the building; C) Roof pitch angle layer (image); D) Roof orientation layer (image); E) Exposure level layer (image), where light green pixels are feasible areas to setup PV panels with a high solar exposure, dark green pixels are low feasibility areas to setup PV panels or areas with a low solar exposure, red pixels are surfaces with discontinuities greater than one meter; F) Approximate surface area; *C) Normalized radiation levels of Fig. 3 corresponding to each roof pitch (in color), roof pitch angles distribution and RPI score; *D) Normalized radiation levels of Fig. 4 corresponding to each orientation (in color), roof orientations distribution and OI score; *E) Exposure level distribution and FEI score; TOTAL) Topology Indicator score ($I_2$).

### 5.3. Aggregation of flexible and topology indicators

The results obtained for the users involved in this study are shown in Fig. 11 and Table *VI*. It is interesting to observe the case of User 2, with a high Topology Indicator score but a low Flexible Indicator score. Applying a standard geometric mean, this user would get a 0.49 (not recommended for installing PV panels), whereas applying a hybrid aggregation, this same user would get a 0.55 (recommended for installing PV panels). This case shows a critical scenario in which hybrid aggregation might produce a more reasonable result than a standard geometric mean.

## 6. Conclusion

This paper targets two audiences. First, for those interested in identifying the flexibility potential of a set of users. This methodology presents different indicators and discusses why a single indicator is not enough to determine a user's flexibility potential. Using these indicators, edge technologies with recommender systems could develop local recommendations, and training stages of ML algorithms could also easily tag the consumptions they are studying for future recommendations. Second, for those interested in calculating the solar potential of an area to determine the best feasible locations to install PV panels. Finally, both indicators are combined to jointly assess the feasibility and suitability of panel installation in a rigorous yet straightforward manner. The aggregation of both indicators is the most significant contribution of this study, which has not yet been addressed in the literature. The indicators proposed can be used in building energy recommender systems, by public agencies to enhance transition policies, subsidies for the installation of photovoltaic panels for users with flexible energy consumptions; companies to develop marketing campaigns among their clients offering solar panels, solar panels plus battery systems or different tariffs.

This study comprises a group of twelve users from different locations and nature tested through flexibility indicators. The results show how flexible end-users are identified and classified using different temporal aggrupations. In order to show the potential of this approach, representative buildings for those consumptions with multiple and diverse topologies were assessed through cutting-edge technology: high-resolution urban 3D models. Both perspectives are merged into a single indicator through a hybrid approach (arithmetic-geometric), enhancing in a descriptive and intuitive manner the assessment of

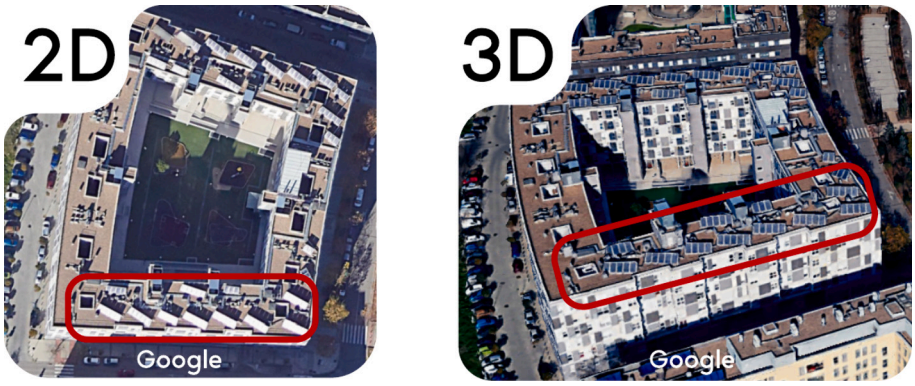


**Fig. 12.** Comparison of satellite images in 2D and the same image obtained from the High-Resolution 3D model.

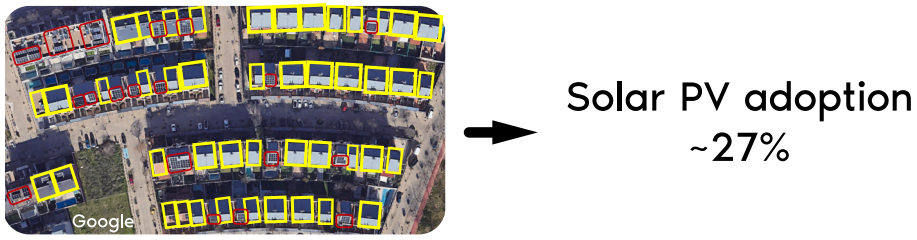


**Fig. 13.** Quantifying Solar PV Adoption at neighborhood level through Automated Identification of PV Panels (conceptual representation).

suitability and feasibility of potential end-users of PV energy sources, easing the energy transition in urban settings.

The present study shows two potential limitations. The first is associated with possible overestimations or imprecise assessments stemming from the absence of data or insufficient information. This lack of data can be due to low sample rates or missing samples in the load monitoring time series that might require additional adjustments in selecting time windows, threshold levels, etc., to adjust the assessment according to the missing data. The lack of data on the topological evaluation could imply that not all available surfaces are appropriate for installing PV panels. For instance, a surface must meet some structural requirements that cannot be evaluated from satellite images but must be assessed in situ and follow the norms and standards established within each respective country.

A second limitation is related to the need of a sub-group analysis to adjust parameters or time windows. For instance, when comparing an industrial setting with a group of residential consumers, the differences among residential clients are smaller due to the use of large values corresponding to parameters supporting industrial features. For additional characterizations, a separate analysis can be conducted using the same indicators, adjusting the levels as needed.

One promising future contribution is to consider integrating the potential carbon emission reduction associated with green electricity usage as part of the current Suitable Indicator. Including this new dimension as part of the Suitable Indicator could enhance end-users identification more akin to this type of energy source. A second prospective research could explore the automated detection of existing PV panels by leveraging the enhanced characterization capabilities of the High-Resolution 3D models. Fig. 12 shows how 3D models not only allow for a better characterization of the topological features but also enhance the depiction of the texture of PV panels installed on the rooftop of a structure.

Another potential future research endeavor related to the previous one could involve developing a novel composite indicator for evaluating Solar PV adoption rates at the regional level based on the PV modules detected on rooftops.

Fig. 13 shows a representation of the concept. This new indicator would aid in gauging and quantifying the energy transition within cities and regions of a country.

## CRediT authorship contribution statement

**Pablo Calvo-Bascones:** Writing – review & editing, Writing – original draft, Validation, Software, Methodology, Formal analysis, Data curation, Conceptualization. **Francisco Martín-Martínez:** Writing – review & editing, Writing – original draft, Visualization, Validation, Software, Methodology, Funding acquisition, Data curation, Conceptualization.

## Declaration of competing interest

The authors declare the following financial interests/personal relationships which may be considered as potential competing interests: Pablo Calvo reports financial support was provided by Horizon 2020 Framework Programme. Francisco Martin-Martinez reports financial support was provided by Horizon 2020 Framework Programme.

## Data availability

Data can be found in reference [42]. If there is any issue with the link, please request this to the authors. It is imperative to handle and process this data in a manner that prioritizes the privacy protection of property owners. The authors declare that all the data in this project have been used only for research purposes without commercial use.

## Acknowledgments

This work was supported by REDREAM project, funded by European Union's Horizon 2020 research and innovation programme (Horizon2020 Framework Programme) under grant agreement number 957837.

## Appendix A. Appendix

This appendix gathers the algorithms for flexible consumption indicators.

**Algorithm 1.** **LEVEL:** Energy Level Indicator

**Algorithm 1 LEVEL:** Energy Level Indicator

**Input**: *C*: Time series containing D days and T values per day of the consumption of a consumer.
**Output**: *ELI*: Energy Level Indicator [0-1]

```
Separate the consumption per day, obtaining a matrix of power Y[1:D] [1:T]
z=0 //Auxiliar variable
Obtain energy per day E[1:D]:
  E[1:D] = sum (Y[1:D][t] for t ∈ [1,...,T])
Define energy levels H, L considering the number of T values used:
for d=1 to D:
        if (E[d]>H)
                z+=1
        else if (E[d]> L)
                z+=E[d]/H
ELI = z/D
return ELI
```

**Algorithm 2.** **CONSISTENCY:** Daily Energy Consistency Indicator

**Algorithm 2 CONSISTENCY:** Daily Energy Consistency Indicator

**Input**: *C*: Time series containing D days and T values per day of the consumption of a consumer.
**Output**: *ECI*: Energy Consistency Indicator [0-1]

```
Separate the consumption per day, obtaining Y[1:D] [1:T]
z=0 //Auxiliary variable
Obtain mean and standard deviation per time:
  M[1:T] = mean (Y[d][1:T] for d ∈ [1,...,D])
  S[1:T] = std (Y[d][1:T] for d ∈ [1,...,D])
Define confidence interval n:
for d=1 to D:
        if (Y[d][t]>M[t]-n·S[t] & M[t]<M[t]+n·S[t]) ∀t
                z+=1
ECI = z/D
return ECI
```

**Algorithm 3.** **CONSISTENCY:** Energy Variation Indicator

**Algorithm 3 CONSISTENCY:** Energy Variation Indicator

**Input**: *C*: Time series containing D days and T values per day of the consumption of a consumer.
**Output**: *EVI*: Energy Variation Indicator [0-1]

```
Apply Algorithm 1 to obtain the energy per day E[1:D]
Obtain standard deviation:
  M = mean (E[1:D])
  S = std (E[1:D])
EVI =0
if (S/M<0.1)
        EVI =1
else if (S<M)
        EVI =1- S/M
return EVI
```

**Algorithm 4.** **VARIATION:** Amplitude Level Indicator

**Algorithm 4 VARIATION:** Amplitude Level Indicator

**Input**: *C*: Time series containing D days and T values per day of the consumption of a consumer.
**Output**: A*LI*: Amplitude Level Indicator [0-1]

```
Obtain quartiles per time window, e.g. hour:
  Q1[1: T] = quartile (25%, C)
  Q3[1:T] = quartile (75%, C)
Calculate range R
  R[1:T]=Q3[1:T] -Q1[1:T]
Define deviation highest power level, H:
z=0 //Auxiliar variable
for t=1 to T:
    if (R[t]>H)
        z+ =1
    else if (R[t]>0.75·H)
        z+ =0.75
    else if (R[t]>0.5·H)
        z+ =0.5
    else if (R[t]>0.25·H)
        z+ =0.25
ALI=z/T
return ALI
```

**Algorithm 5. VARIATION:** Standard Deviation Indicator

**Algorithm 5 VARIATION:** Standard Deviation Indicator

**Input**: *C*: Time series containing D days and T values per day of the consumption of a consumer.
**Output**: *SDI*: Standard Deviation Indicator [0-1]

```
Obtain standard deviation per time window, e.g. hour:
  S[1:T] =std (C)
Define deviation highest power level H:
Define confidence level n
z=0 //Auxiliar variable
for t=1 to P:
    if (S[t]>H)
        z+ =1
    else if (S[t]>0.75·H)
        z+ =0.75
    else if (S[t]>0.5·H)
        z+ =0.5
    else if (S[t]>0.25·H)
        z+ =0.25
SDI =z/T
return SDI
```

## References


[1] European Commission. Energy Performance of Buildings Directive [Online]. Available, https://energy.ec.europa.eu/topics/energy-efficiency/energy-efficient-buildings/energy-performance-buildings-directive_en; 2024 [Accessed: 15-Mar-2024].

[2] Filipović S, Lior N, Radovanović M. The green deal – just transition and sustainable development goals Nexus. Renew Sust Energ Rev Oct. 2022;168:112759. https://doi.org/10.1016/J.RSER.2022.112759.

[3] E. K Schwartz M Krarti, Schwartz EK, Krarti M. "Review of Adoption Status of Sustainable Energy Technologies in the US Residential Building Sector," *Energies* 2022*, Vol. 15, Page 2027*, vol. 15, no. 6, p. 2027. Mar 2022. https://doi.org/10.3390/EN15062027.

[4] Ghaleb B, Asif M. Assessment of solar PV potential in commercial buildings. Renew Energy Mar. 2022;187:618–30. https://doi.org/10.1016/J.RENENE.2022.01.013.

[5] Li R, Dane G, Finck C, Zeiler W. Are building users prepared for energy flexible buildings?—a large-scale survey in the Netherlands. Appl Energy 2017;203:623–34. https://doi.org/10.1016/j.apenergy.2017.06.067.

[6] International Energy Agency. Renewables 2023. 2024.

[7] IEA-PVPS, et al. Snapshot of Global PV Markets. 2020.

[8] Himeur Y, et al. A survey of recommender systems for energy efficiency in buildings: principles, challenges and prospects. Inf Fusion 2021;72(February):1–21. https://doi.org/10.1016/j.inffus.2021.02.002.

[9] Rodríguez-Cuenca F, et al. Probability-Density-Based Energy-Saving Recommendations for Household Refrigerating Appliances. Eng Proc 2023. https://doi.org/10.3390/ENGPROC2023039043. *Vol. 39, Page 43*, vol. 39, no. 1, p. 43, Jul. 2023.

[10] Luo F, Ranzi G, Kong W, Liang G, Dong ZY. Personalized residential energy usage recommendation system based on load monitoring and collaborative filtering. IEEE Trans Ind Informatics 2021;17(2):1253–62. https://doi.org/10.1109/TII.2020.2983212.

[11] Bobadilla J, Ortega F, Hernando A, Gutiérrez A. Recommender systems survey. Knowl-Based Syst Jul. 2013;46:109–32. https://doi.org/10.1016/J.KNOSYS.2013.03.012.

[12] Rashid H, Singh P, Ramamritham K. "Revisiting selection of residential consumers for demand response programs," *BuildSys* 2017 - *Proc. 4th ACM Int. Conf. Syst. Energy-Efficient Built Environ.*, vol. 2017-Janua, no. 2, pp. 0–3. 2017. https://doi.org/10.1145/3137133.3137157.

[13] Rusche S, Weissflog J, Wenninger S, Häckel B. How flexible are energy flexibilities? Developing a flexibility score for revenue and risk analysis in industrial demand-side management. Appl Energy 2023;345(June). https://doi.org/10.1016/j.apenergy.2023.121351.

[14] Yang S, et al. Flexibility index for a distributed energy system design optimization. Renew Energy 2023;219(P1):119423. https://doi.org/10.1016/j.renene.2023.119423.

[15] Sánchez-Aparicio M, Martín-Jiménez J, Del Pozo S, González-González E, Lagüela S. "Ener3DMap-SolarWeb roofs: A geospatial web-based platform to compute photovoltaic potential," *Renew. Sustain. Energy Rev.*, vol. 135, no. August 2020, pp. 1–14. 2021. https://doi.org/10.1016/j.rser.2020.110203.
[16] Mahaya C, Zemmouri N, Benharra H, Elnokaly A. Solar access assessment in semi-arid urban context: an application study for ten urban forms of existing apartment buildings districts in Batna City, Algeria. Sustain Cities Soc 2022;83, no. March: 103909. https://doi.org/10.1016/j.scs.2022.103909.
[17] Bienvenido-Huertas D, Farinha F, Oliveira MJ, Silva EMJ, Lança R. Comparison of artificial intelligence algorithms to estimate sustainability indicators. Sustain Cities Soc 2020;63(May). https://doi.org/10.1016/j.scs.2020.102430.
[18] Puente C, Palacios R, González-Arechavala Y, Sánchez-Úbeda EF. Non-intrusive load monitoring (NILM) for energy disaggregation using soft computing techniques. Energies 2020;13(12):1–20. https://doi.org/10.3390/en13123117.
[19] Dash S, Sahoo NC. Electric energy disaggregation via non-intrusive load monitoring: a state-of-the-art systematic review. Electr Power Syst Res 2022;213, no. February:108673. https://doi.org/10.1016/j.epsr.2022.108673.
[20] Kumar NM, Islam S, Podder AK, Selim A, Bajaj M, Kamel S. Lifecycle-based feasibility indicators for floating solar photovoltaic plants along with implementable energy enhancement strategies and framework-driven assessment approaches leading to advancements in the simulation tool. Front Energy Res 2023;11(February). https://doi.org/10.3389/fenrg.2023.1075384.
[21] AL-Zoubi OH, Al-Tahaineh H, Damseh RA, AL-Zubi AH, Odat S, Shbool B. Evaluating the real-world performance of vertically installed bifacial photovoltaic panels in residential settings: empirical findings and implications. Int J Low-Carbon Technol 2024;19:386–442. https://doi.org/10.1093/ijlct/ctad138.
[22] Machidon D, Istrate M. Tilt angle adjustment for incident solar energy increase: a case study for Europe. Sustain 2023;15(8). https://doi.org/10.3390/su15087015.
[23] Phadnis N, Yang RJ, Wijeratne PU, Zhao H, Liu C. The impact of solar PV design tilt and orientation on project values. Smart Innov Syst Technol 2019;131:301–10. https://doi.org/10.1007/978-3-030-04293-6_30.
[24] Che Y, Li X, Liu X, Zhang X. Characterizing the 3-D structure of each building in the conterminous United States. Sustain Cities Soc 2024;105, no. February:105318. https://doi.org/10.1016/j.scs.2024.105318.
[25] Ni P, Yan Z, Yue Y, Xian L, Lei F, Yan X. Simulation of solar radiation on metropolitan building surfaces: a novel and flexible research framework. Sustain Cities Soc 2023;93, no. March:104469. https://doi.org/10.1016/j.scs.2023.104469.
[26] Yildirim D, Büyüksalih G, Şahin AD. Rooftop photovoltaic potential in Istanbul: calculations based on LiDAR data, measurements and verifications. Appl Energy 2021;304(August). https://doi.org/10.1016/j.apenergy.2021.117743.
[27] Hong T, Lee M, Koo C, Kim J, Jeong K. Estimation of the available rooftop area for installing the rooftop solar photovoltaic (PV) system by analyzing the building shadow using Hillshade analysis. Energy Procedia 2016;88:408–13. https://doi.org/10.1016/j.egypro.2016.06.013.
[28] López-Fernández L, Lagüela S, Picón I, González-Aguilera D. Large scale automatic analysis and classification of roof surfaces for the installation of solar panels using a multi-sensor aerial platform. Remote Sens 2015;7(9):11226–48. https://doi.org/10.3390/rs70911226.
[29] Liu J, et al. A novel approach for assessing rooftop-and-facade solar photovoltaic potential in rural areas using three-dimensional (3D) building models constructed with GIS. Energy 2023;282, no. April:128920. https://doi.org/10.1016/j.energy.2023.128920.
[30] Sun X, et al. GABLE: a first fine-grained 3D building model of China on a national scale from very high resolution satellite imagery. Remote Sens Environ 2024;305, no. February:114057. https://doi.org/10.1016/j.rse.2024.114057.
[31] Waqas H, et al. Enhancement of the energy performance of an existing building using a parametric approach. J Energy Eng Nov. 2022;149(1):04022057. https://doi.org/10.1061/JLEED9.EYENG-4546.
[32] Gong FY, Zeng ZC, Ng E, Norford LK. Spatiotemporal patterns of street-level solar radiation estimated using Google street view in a high-density urban environment. Build Environ 2019;148(January):547–66. https://doi.org/10.1016/j.buildenv.2018.10.025.
[33] Liang J, Gong J, Xie X, Sun J. Solar3D: an open-source tool for estimating solar radiation in urban environments. ISPRS Int J Geo-Information 2020;9(9). https://doi.org/10.3390/ijgi9090524.
[34] Ilba M. Estimating the daily solar irradiation on building roofs and facades using blender cycles path tracing algorithm. E3S Web Conf 2016;10. https://doi.org/10.1051/e3sconf/20161000027.
[35] Leroux F, Germain M, Clabaut É, Bouroubi Y, St-Pierre T. Improving three-dimensional building segmentation on three-Dimensional City models through simulated data and contextual analysis for building extraction. ISPRS Int J Geo-Information 2024;13(1). https://doi.org/10.3390/ijgi13010020.
[36] OECD. Handbook on constructing composite indicators. 2008.
[37] Huld TA, Súri M, Dunlop ED, Albuisson M, Wald L. "Integration of HELIOCLIM-1 Database Into PV-GIS to Estimate Solar Electricity Potential in Africa," *20th Eur. Photovolt. Sol. Energy Conf. Exhib.*, no. June 2014, p. 2989. 2005.
[38] Zhao P, Ali Z, Ahmad Y. Developing indicators for sustainable urban regeneration in historic urban areas : Delphi method and analytic hierarchy process ( AHP ). Sustain Cities Soc 2023;99, no. September:104990. https://doi.org/10.1016/j.scs.2023.104990.
[39] Hély V, Antoni JP. "Combining indicators for decision making in planning issues: A theoretical approach to perform sustainability assessment," *Sustain. Cities Soc.*, vol. 44, no. November 2018, pp. 844–854. 2019. https://doi.org/10.1016/j.scs.2018.10.035.
[40] Abbasi MH, Abdullah B, Castaño-Rosa R, Ahmad MW, Rostami A. A framework to identify and prioritise the key sustainability indicators: assessment of heating systems in the built environment. Sustain Cities Soc 2023;95(May). https://doi.org/10.1016/j.scs.2023.104629.
[41] European Commission, "H2020-Real consumer engagement through a new user-centric ecosystem development for end-users' assets in a multi-market scenario. Grant agreement ID: 957837," 2023. [Online]. Available, https://redream-energy-network.eu/ [Accessed: 12-Jul-2023].
[42] Calvo P, Martín-Martínez F. Data source and results [Online]. Available, https://upcomillas-my.sharepoint.com/:f:/g/personal/fmartin_comillas_edu/Eph_ZtGBlIJJqn2Yixj5jywBnQFE4swFeu5s9unHyUb0wA?e=k64rGj; 2023.